Silicon-Wafer Based Planar Models for Hydrotreating Catalysts

E. J. M. HENSEN, L. COULIER, A. BORGNA, J. A. R. van VEEN and J. W. NIEMANTSVERDRIET

Schuit Institute of Catalysis, Eindhoven University of Technology, P.O. Box 513, 5600 MB Eindhoven (The Netherlands)

E-mail: e.j.m.hensen@tue.nl

Abstract

In the present study the use of planar silicon-based models for hydrotreating catalysts is discussed. The specific flat nature makes these models amenable to high resolution surface-sensitive techniques such as XPS. The additional possibility to measure the activity of such model catalysts in thiophene hydrodesulfurization provides a powerful tool to determine structure-activity relations. Here, we study the effect of chelating agents (NTA and EDTA) on the sulfidation order of NiMo catalysts. The XPS results clearly show that the use of these chelating agents retards the sulfidation of Ni with respect to Mo. Especially, EDTA is effective by postponing Ni sulfidation after Mo is completely sulfided. The latter catalyst also displays the highest activity which is attributed to the highest amount of 'Ni-Mo-S'-type phases. In essence, the results underpin the notion that such 'Ni-Mo-S' phase can be formed effectively when Ni sulfidation proceeds after MoS_2 has been formed. When Ni sulfides at too low temperature, inactive bulky Ni_3S_2 clusters are formed.

INTRODUCTION

General

Supported mixed transition metal sulfide catalysts play a pivotal role in refineries for the production of clean motor fuels. They are employed not only to hydrotreat the final products like gasoline and diesel, but also to pretreat fluid catalytic cracking or reformer feed [1]. Furthermore, they provide the hydrogenation functionality in most hydrocracking catalysts that upgrade vacuum residue to more valuable products.

Two major drivers for the development of more active hydrotreating catalysts are (i) dwindling oil supplies forcing refiners to use heavier feedstock and (ii) ever-tightening motor fuel specifications (for instance, the EU Auto Oil programme II [2]). Noteworthy is that mostly the use of an improved catalyst is more economic than modifications to the process.

In addition to the demand for more active catalysts, selectivity is also an issue to consider. Whereas the desulfurization of gasoline is not a difficult task in itself due to the thiophenic nature of the sulfur compounds, concomitant olefin hydrogenation leads to a dramatic loss in octane rating when aiming at very low sulfur levels. Here, there is room for the development of catalysts with an increased hydrodesulfurization/hydrogenation ratio [3, 4]. For the near future, the introduction of the fuel cells in mobile applications may set zero sulfur limits when oil-derived fuels are to be used to generate hydrogen via onboard partial oxidation [5].

While research on hydrotreating catalysts has been extensive over the last 50 years [6–11], it has proven very difficult to relate catalyst structure to catalyst activity and selectivity on the molecular level. Partly, this is to be attributed to the heterogeneous nature of such catalysts in the sense that various metal sulfide phases are present.

In recent years, we have employed the model catalyst approach to heterogeneous catalysis. The essential point is to prepare planar model catalysts by spincoating which mimics

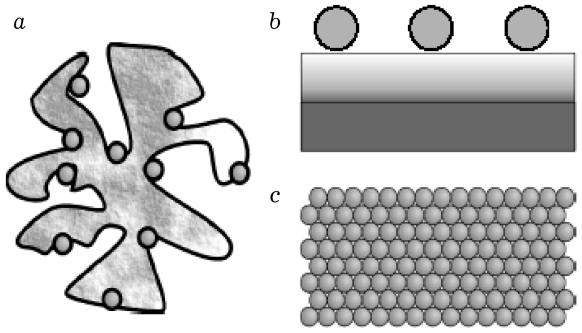

Fig. 1. Schematic drawing of a porous catalyst (*a*), a flat supported model catalyst (*b*) and a single crystal (*c*).

the industrial pore volume impregnation method. In this way, realistic models can be obtained which are easily amenable to high-resolution spectroscopic studies. The specific catalytic activity of such well-defined models can also be evaluated. Here, we will show that the strong tandem-mix of characterization and reactivity evaluation of these realistic models enables one to obtain detailed insight into the relation between sulfidation behavior of the transition metals and their activity.

Preparation of model catalysts

Models of catalysts are used to circumvent the disadvantages of industrial catalysts (Fig. 1). The ultimate and most simple model is a well-defined single crystal surface. These single crystals have been used successfully in ultra high vacuum (UHV) to study fundamental adsorption behaviour of molecules on metal surfaces and its dependence on surface geometry and composition. A major drawback of single crystal surfaces is the so-called pressure- and material-gap with respect to industrial catalysts. Planar silicon-based model catalysts provide opportunities to bridge these gaps. These models consist of a flat model support covered by the precursor material. The model support is made up by a thin layer of SiO_2 or Al_2O_3 on a conducting substrate. The precursor material can be applied by evaporation, electron beam lithography or wet chemical preparation [12]. Especially the latter method has gained increasing importance. Spincoating introduced by Kuipers *et al.* [13] mimics the widely applied pore-volume impregnation used on the industrial scale and allows full control over the loading (Fig. 2) [14].

Due to the non-porous conducting support all active particles are on top of the substrate and are thus 'visible' for various surface sensitive techniques. Furthermore, charging phenomena during electron- or ion-spectroscopies are largely eliminated due to the conducting substrate. The absence of pores allows the measurements of intrinsic kinetics without effects of diffusion limitations due to small pore sizes. The majority of studies on model catalysts concern the 'classic' metals on oxidic supports. However, recently model catalysts have also been applied in different fields of catalysis such as polymerization [15] and transition metal oxide and sulfide catalysts [16]. An excellent review on the preparation and applications of model supports and catalysts has been published by Gunter *et al.* [12].

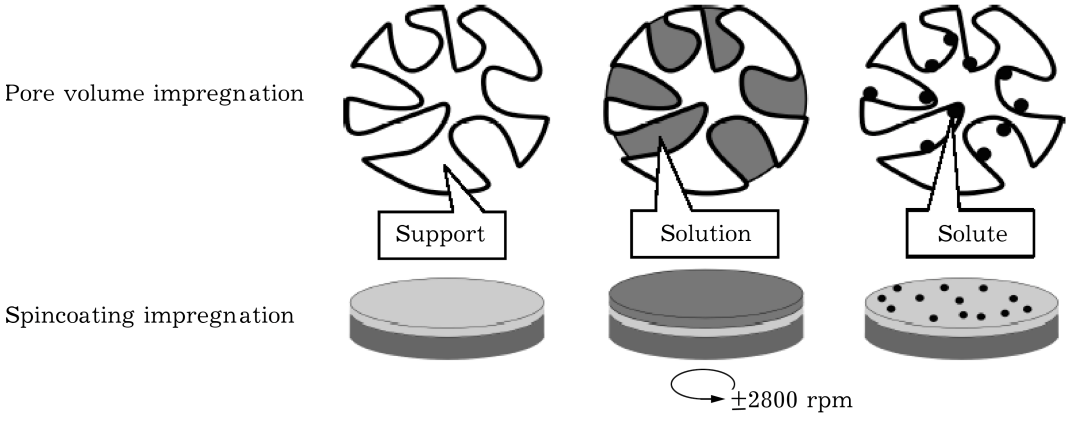

Fig. 2. Analogy between the spincoating technique used for model catalysts in this thesis and impregnation of a porous catalyst.

Characterization by X-ray photoelectron spectroscopy

Where in industrial practice the feed is spiked with sulfur-containing molecules to slowly convert catalyst precursors to their active sulfided form, a mixture of hydrogen sulfide and hydrogen is generally applied in laboratory practice. The group of Niemantsverdriet [17, 18] has used the model catalyst approach to study the sulfidation of SiO_2-supported MoO_3 in great detail. X-ray photoelectron spectroscopy is an ideal tool [19] to study this transformation since essential information of the different types of molybdenum and sulfur species can be obtained. It was found that the sulfidation of Mo occurred via Mo^{5+}-oxysulfides and that no MoO_2 or elemental sulfur was involved, as proposed by Arnoldy *et al.* [20]. More recently, de Jong *et al.* [16] prepared CoMo-NTA/Al_2O_3 and CoMo-NTA/SiO_2 model catalysts and concluded that these catalysts exhibit activities and product distributions for thiophene HDS similar to those of their high surface area counterparts.

Reactivity evaluation

Thiophene is one of the most used model compounds for studying hydrodesulfurization reactivity. Despite intensive research (see [21–23]) there is still debate on the exact reaction mechanism. The possible reaction paths for thiophene HDS are collected in Fig. 3. Direct C–S cleavage was proposed by Lipsch and Schuit [24], whereas others [25, 26] have proposed partially hydrogenated intermediates, *i. e.* tetrahydrothiophene (THT) or dihydrothiophenes (DHT), which are very difficult to observe under standard reaction conditions [27]. Recently, low temperature experiments by Hensen *et al.* [28, 29] provided evidence for DHTs and THT as intermediates in thiophene HDS.

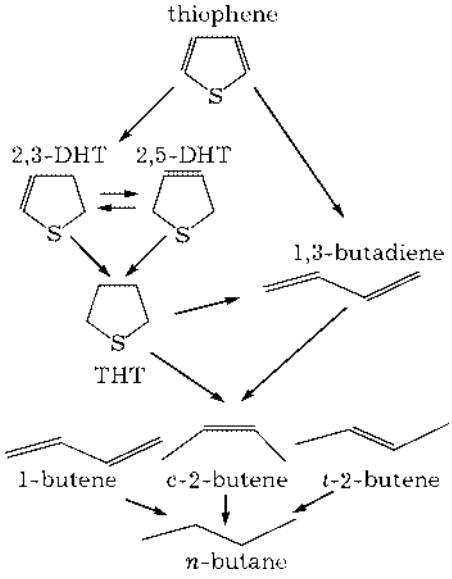

Fig. 3. Possible reaction pathways for the desulfurization of thiophene.

EXPERIMENTAL

Preparation of model catalysts

A silica model support was prepared by oxidizing a Si (100) wafer with a diameter of 75 mm in air at 750 °C for 24 h. Rutherford back scattering (RBS) measurements indicated that the SiO_2 layer is about 90 nm thick. The roughness of the SiO_2 surface is below 5 Å as derived from AFM experiments. After oxidation the wafer was cleaned in a solution of ammonia and hydrogen peroxide at 65 °C for 10 min. The surface was rehydroxylated by boiling in water for 30 min. Cobalt and molybdenum were applied by spincoating the SiO_2/Si (100) wafers at 2800 rpm in N_2 with aqueous solutions of cobalt nitrate ($Co(NO_3)_2 \cdot 6H_2O$, Merck) and ammonium heptamolybdate ($(NH_4)_6Mo_7O_{24} \cdot 4H_2O$, Merck), respectively. The concentration of Co and Mo in the aqueous solutions was adjusted to result in a loading of 2 Co atoms/nm^2 and 6 Mo atoms/nm^2 after spincoating, which was checked by RBS. The mixed phase model catalysts were prepared by spincoating with aqueous solutions containing Co and Mo with an atomic ratio of 1 : 3, respectively. Catalysts containing nitrilo triacetic acid (NTA) were prepared by spincoating ammoniacal solutions containing ammonium heptamolybdate (Merck), cobalt nitrate and NTA (Acros Organics) as described by van Veen *et al.* [30]. The NTA solutions contained Co:Mo:NTA ratios of 1 : 3 : 4. Calcination was carried out in a glass reactor under a 20 % vol. O_2 in Ar flow at 1.5 bar. The catalysts were heated to 500 °C at a rate of 5 °C/min and kept at the desired

temperature for 30 min. Sulfidation of the model catalysts was carried out in a glass tube reactor with a mixture of 10 % vol. H_2S in H_2 at a flow rate of 60 ml/min. The catalysts were heated at a rate of 5 °C/min (NTA-containing samples: 2 °C/min) to the desired temperature and kept there for 30 min. After sulfidation, the reactor was cooled to room temperature under a helium flow and brought to the glovebox, where the model catalyst was mounted in a transfer vessel for transport to the XPS under N_2 atmosphere.

RESULTS

XPS characterization

The sulfidation behaviour of molybdenum was described in earlier reports [16–18, 31, 32]. Briefly, the sulfidation of Mo proceeds at moderate temperatures, starting around 50 °C. Complete transformation to MoS_2 occurs at temperatures above 150 °C. The Mo 3*d* spectra of the catalysts sulfided at intermediate temperatures can be all interpreted in terms of Mo^{6+}, Mo^{5+} and Mo^{4+} doublets as described earlier [16, 17]. Addition of chelating agents in the preparation stage did not affect the sulfidation behaviour of Mo significantly.

Figure 4 shows the Ni 2*p* and S 2*p* spectra during progressive sulfidation of a calcined NiO_x/SiO_2 model catalyst. The Ni 2*p* spectrum of the calcined catalyst shows the characteristic pattern of oxidic nickel with a Ni $2p^{3/2}$ peak at 856.8 eV and a shake up feature at higher binding energy [33]. The binding energy of 856.8 eV corresponds well with that of Ni_2O_3 [33]. Sulfidation at room temperature shows the appearance of a second doublet at lower binding energy. At higher temperatures this doublet increases in intensity, while the doublet with Ni $2p^{3/2}$ at 856.8 eV decreases and finally disappears at temperatures above 50 °C. The Ni $2p^{3/2}$ peak at 853.8 eV obtained after sulfidation at 400 °C corresponds well with that of bulk Ni_3S_2 [33]. Sulfur is present in the S^{2-} state as derived from the binding energy of 161.8 eV. Ni 2*p* spectra of a Ni-EDTA/SiO_2/Si model (not shown) show that the sulfidation of Ni is retarded to temperatures above 200 °C.

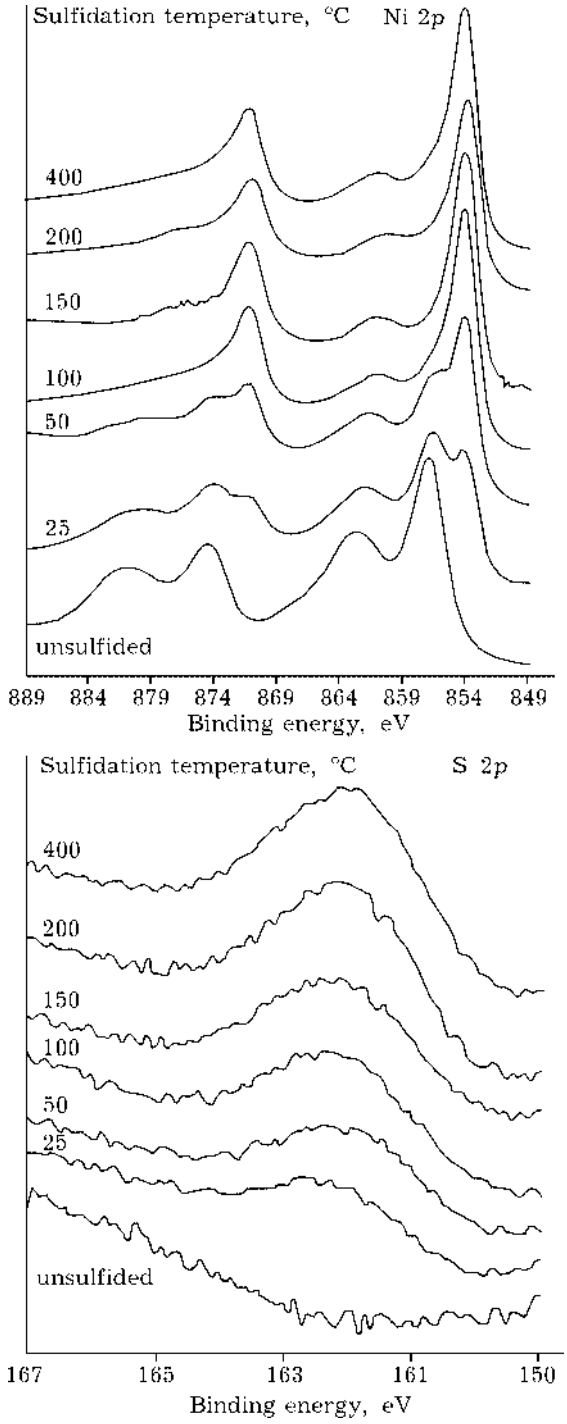

Fig. 4. Ni 2*p* and S 2*p* spectra of calcined NiO_x/SiO_2/Si(100) sulfided in 10 % H_2S/H_2 for 30 min at various temperatures.

The sulfidation is complete at 300 °C. N 1*s* spectra indicate that EDTA decomposes at temperatures above 200 °C.

Figure 5 shows the Ni 2*p* and Mo 3*d* spectra of $NiMo/SiO_2$ at various sulfidation stages. The Mo 3*d* spectra are identical to those of

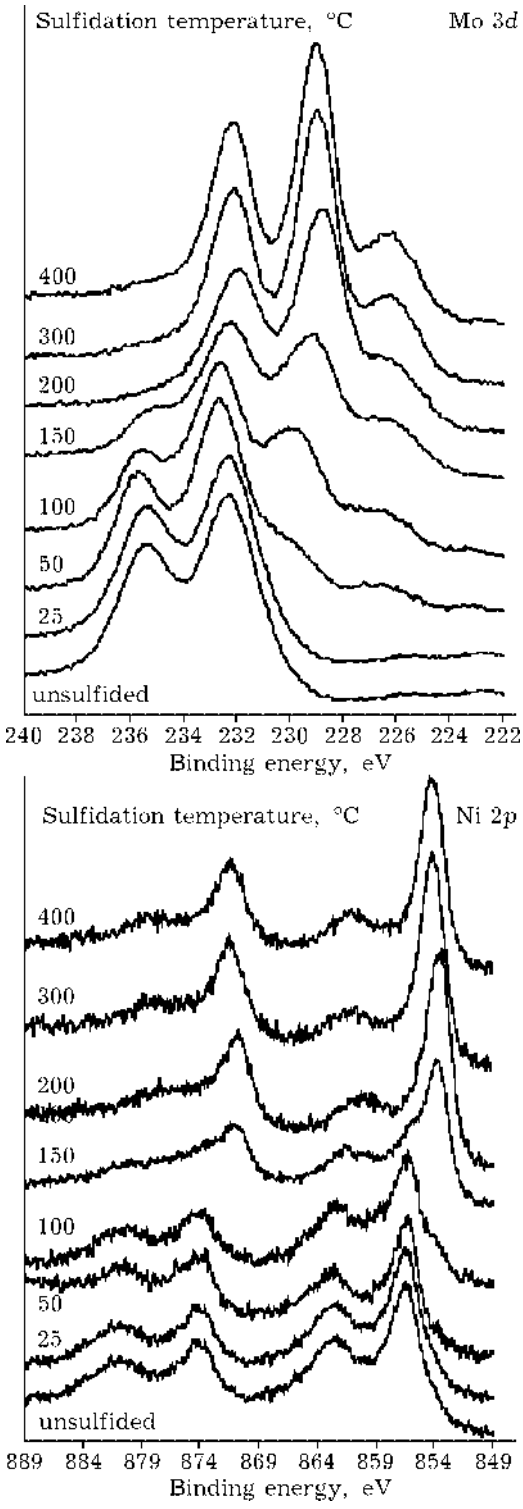

Fig. 5. Ni 2*p* and Mo 3*d* spectra of calcined $NiMo/SiO_2/Si(100)$ sulfided in 10 % H_2S/H_2 for 30 min at various temperatures.

Mo/SiO_2 [31]. However, the Ni 2*p* spectra reveal a much slower conversion of nickel oxide to the sulfided state than for Ni/SiO_2. Ni sulfidation only starts at temperatures around 100 °C, which is some 75 °C higher than for the calcined Ni/SiO_2. At these temperatures a second doublet with small shake up features appears at a Ni $2p^{3/2}$ binding energy of 854.2 eV. Above 150 °C the sulfidation is complete. A small, but significant higher binding energy for sulfided Ni in $NiMo/SiO_2$ compared to that of Ni/SiO_2 is observed. Comparing Ni and Mo, one observes that the rates of sulfidation are similar, *i. e.* starting around 50 °C and being complete between 150 and 200 °C. The XP spectra of uncalcined $NiMo/SiO_2$ catalysts (not shown) are similar to those of the single-phase catalysts. Sulfidation of Ni precedes that of Mo, although the temperature regime where sulfidation occurs shows some overlap.

Figure 6 shows the Ni 2*p* and Mo 3*d* spectra of a NiMo-EDTA/SiO_2 model catalyst. The Mo 3*d* spectrum of the fresh catalyst shows one doublet with a Mo $3d^{5/2}$ binding energy of 232.2 eV characteristic of molybdenum complexated to chelating agents. The sulfidation behaviour of Mo is identical to that of Mo in Mo/SiO_2 and $NiMo/SiO_2$. The doublet with Mo $3d^{5/2}$ binding energy at 229.0 eV is characteristic for MoS_2. The Ni 2*p* spectra show that EDTA retards the sulfidation of Ni significantly. The spectrum of the fresh catalyst shows a single doublet with Ni $2p^{3/2}$ at 856.1 eV, corresponding to Ni complexed to EDTA, and shake up features at higher binding energy. Sulfidation does not start until temperatures around 200 °C where a second doublet at lower binding energy appears. Ni sulfidation is complete at 300 °C. The same sulfidation behaviour was observed for Ni-EDTA/SiO_2 catalysts. Note however that the Ni $2p^{3/2}$ binding energy of the sulfided Ni in NiMo-EDTA/SiO_2, *i. e.*, 854.1 eV, is 0.3 eV higher than that of the fully sulfided Ni-EDTA/SiO_2 catalyst, *i. e.*, 853.8 eV.

The sulfidation behavior of a NiMo-NTA/SiO_2/Si(100) model catalyst was studied in a similar way (spectra not shown here). While Mo sulfidation proceeded qualitatively in the same way as in NiMo-EDTA/SiO_2 and NiMo/SiO_2, Ni sulfidation is faster than in the EDTA case and starts already at 125 °C. This corresponds well with the sulfidation of Co in a CoMo-NTA/SiO_2 model catalyst [31]. In contrast to the EDTA case, there exists an overlap

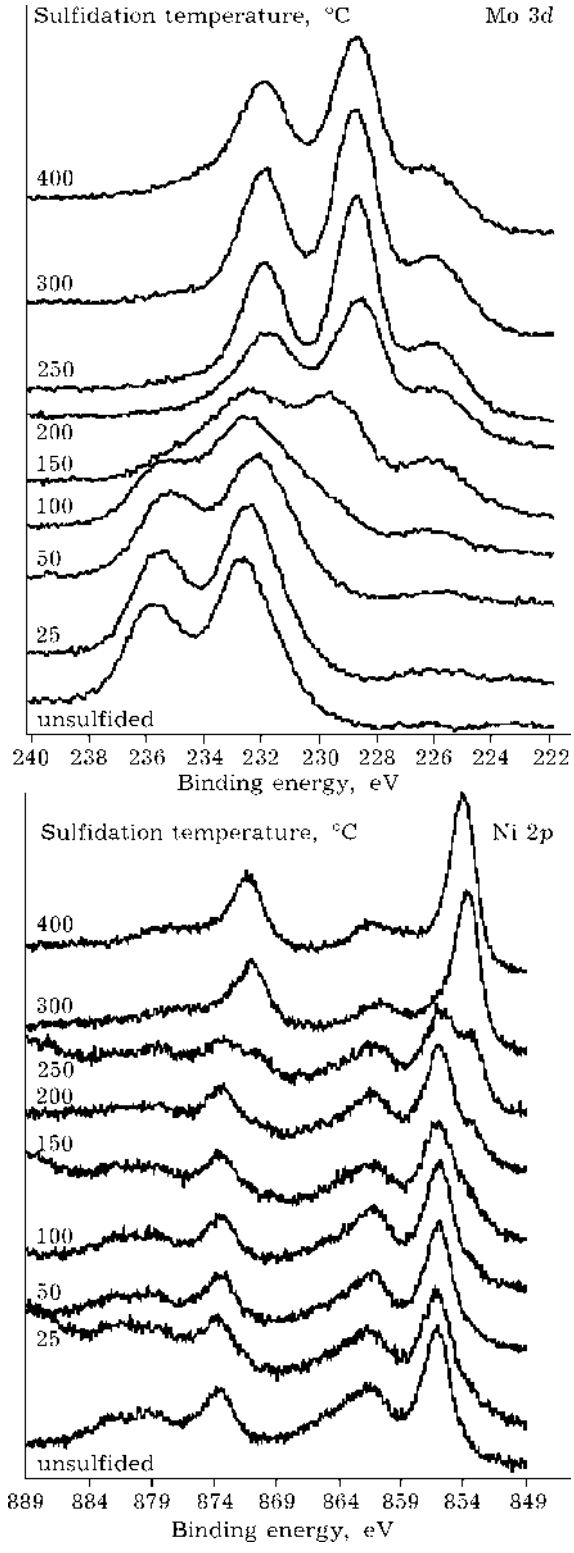

Fig. 6. Ni 2*p* and Mo 3*d* spectra of calcined NiMo-EDTA/SiO_2/Si(100) sulfided in 10 % H_2S/H_2 for 30 min at various temperatures.

in temperature where Ni and Mo are converted to their sulfided state. The Ni $2p^{3/2}$ binding energy of the nickel in the sulfidic state (854.2 eV) equals that in NiMo-EDTA/SiO_2 and differs from that of bulk nickel sulfide.

TABLE 1

Thiophene conversion after 60 min at 400 °C in batch reactor

Catalyst	Conversion, %
Mo/SiO_2/Si	0.2
NiMo-uncalcined/SiO_2/Si	0.7
NiMo-calcined/SiO_2/Si	1.1
NiMo-NTA/SiO_2/Si	3.5
NiMo-EDTA/SiO_2/Si	6.4

Hydrodesulfurization activity measurements

Table 1 compares the thiophene HDS activities of the various model catalysts. The activity is expressed as yield of products per 5 cm^2 of catalyst after 1 h of batch reaction at 400 °C and has been corrected for blank measurements (bare silica support and empty reactor).

The activity of Ni/SiO_2 corresponds to a pseudo turnover frequency of 1.8 10^{-3} mol thiophene per mol Ni per second. Similar low activities were also found for Ni/SiO_2 and Ni-EDTA/SiO_2 (not shown). The activities of Mo/SiO_2 and Mo-NTA/SiO_2 were similar. The addition of Ni to such catalysts clearly points to the known synergy between these two metals. The activity of calcined NiMo/SiO_2 is higher then that of uncalcined NiMo/SiO_2, which we attribute to an increase in Ni–Mo interaction due to calcination. The highest activities are observed in NiMo/SiO_2 catalysts prepared with chelating agents. NiMo-EDTA/SiO_2 is the most active one amongst the studied catalysts.

DISCUSSION

It is generally accepted that the high activity in CoMo sulfide catalysts derives from the presence of 'Co-Mo-S' type phases. This phase is thought to be present as MoS_2 slabs with Co species located at their edges. Although not proven beyond doubt, 'Ni-Mo-S' analogues of these phases have been proposed [34–36]. Next to these mixed transition metal sulfide phases, also segregated metal sulfides, *i. e.* MoS_2 and Ni_3S_2 may be present with a considerable low-

er activity. The amount of the different phases will strongly depend on the preparation procedure and the sulfidation mechanism. We will discuss the sulfidation mechanism of the model catalysts under study. While small Ni-sulfide species are mobile and able to adsorb on MoS_2 slabs resulting in 'Ni-Mo-S'-type particles, it is expected that large bulky Ni_3S_2 particles redisperse more difficult. In that sense, it appears that sulfidation of Mo prior to Ni leads to a higher amount of 'Ni-Mo-S' phase.

Ni/SiO_2. Ni sulfidation proceeds through progressive oxygen-sulfur exchange. The transformation to the sulfided state is clearly indicated by the shift in the binding energy to lower values. Sulfidation starts already at room temperature and is completed around 100 °C. The resulting phase is most probably Ni_3S_2 and presents a low activity for thiophene HDS. The addition of EDTA hardly affects the thiophene HDS activity, although Ni sulfidation is considerably retarded to higher temperatures.

Mo/SiO_2. Mo sulfidation takes place at moderate temperatures and through different intermediates [17, 31]. The sulfidation mechanism proceeds by O−S exchange transforming oxidic Mo into MoS_2. In the intermediate temperature range Mo^{5+} and oxysulfide species are present [32, 37]. These MoS_2 slabs are active in thiophene HDS. No significant differences in activity were found between uncalcined and calcined Mo catalysts. Here, we should note that an alternative explanation for the chelating ligand effect is a decreased Mo-support interactions as forwarded for alumina-supported catalysts [10, 38]. On the other hand, silica displays a much lower Mo-support interaction which probably makes this effect of minor importance.

$NiMo/SiO_2$. The Ni 2*p* and Mo 3*d* XP spectra of uncalcined $NiMo/SiO_2$ are similar to those of the single phase Ni and Mo catalysts. Since no calcination took place, the metals are not in combined phases. Ni sulfidation clearly precedes Mo sulfidation apart from some small overlap. We surmise that the amount of 'Ni-Mo-S' phase is not optimal since part of the nickel will form Ni_3S_2 phases. Although this appears to be of overriding importance, one notes that small Ni-sulfide clusters may redisperse and form 'Ni-Mo-S' and 'Ni-W-S' phases. Calcination of $NiMo/SiO_2$ prior to sulfidation results in a more active catalyst. Interestingly, the XP spectra show that Ni sulfidation is retarded to higher temperatures and starts around 100 °C and being complete around 200 °C. We attribute this to a Ni-Mo interaction, which hinders low temperature Ni sulfidation. Similar results were obtained for $CoMo/SiO_2$ model catalysts [31]. Based on XP spectra of a reference $NiMoO_4$ sample, we can exclude that this compound is formed upon calcination. Nickel molybdate has been suggested to be an ineffective precursor for 'Ni-Mo-S' type phases [39]. Although Mo sulfidation still lags behind that of Ni, there is a significantly larger temperature range where Ni and Mo sulfide simultaneously, with a greater chance to form the desired 'Ni−Mo−S' phase. This explains the higher activity of the calcined $NiMo/SiO_2$ catalyst.

NiMo-EDTA/SiO_2. Ethylene diamine tetraacetic acid (EDTA) − known to form very stable complexes with ions of nickel and cobalt [40] − is the most successful chelating agents with respect to stabilizing nickel against sulfidation. Whereas Mo sulfidation is similar to that of Mo/SiO_2, the sulfidation of Ni is effectively retarded to temperatures above 200 °C. Hence, all Mo is present as MoS_2 when the sulfidation of Ni starts. In our simple model, this represents an ideal situation for the formation of a maximum amount of 'Ni-Mo-S' phase. This agrees with the highest thiophene HDS activity for the catalysts under study. The activity is almost two times higher than that of NiMo-NTA/SiO_2. This is in qualitative agreement with Prins *et al.* [41, 42]. Although we surmise that the sulfidation order is most important with respect to the final activity, we cannot exclude that the chelating agents have some effect on the dispersion of MoS_2 particles as well, although one generally observes that NTA addition leads to a somewhat larger MoS_2 crystallite size. A general observation is that there is still a lack of a reliable method to determine the edge dispersion of these catalysts.

NiMo-NTA/SiO_2. Adding NTA to the impregnating solution leads to complexation of Ni and stabilizes Ni against low temperature sulfidation, whereas Mo sulfidation is not strongly affected by the NTA ligands. This leads to a large overlap of Mo and Ni sulfidation (results not shown). In fact, Ni sulfidation starts around

75 °C and is completed at about 200 °C. This means that both Ni and Mo sulfidation are essentially completed at the same temperature. Although this would provide more efficient 'Ni-Mo-S' formation than in the NTA-free case, it will probably form a lower amount of such species than in the EDTA case. A similar NTA effect was observed earlier for a $CoMo/SiO_2$ model catalysts [13, 14]. The activity of NiMo-NTA/SiO_2 is indeed between those of NiMo/SiO_2 and NiMo-EDTA/SiO_2.

CONCLUSION

Planar model catalysts offer new possibilities to study the sulfidation mechanism of hydrotreating catalysts in detail. Combined XPS and thiophene HDS measurements applied to a series of NiMo-based model catalysts on a flat silica support allow one to correlate the sulfidation order of the respective transition metals with their activity. Conventional impregnation leads to a low activity catalyst in which Ni sulfidation proceeds at lower temperatures than Mo. Chelating agents are effective in retarding Ni sulfidation. EDTA is most effective and yields the most active catalyst. It is proposed that in order to form a high amount of the active 'Ni-Mo-S' phase, Mo has to be sulfided to MoS_2 to accommodate small Ni-sulfide particles. If Ni sulfidation takes place at too low temperature, bulky Ni_3S_2 particles are formed with low activity, which are not able to redisperse on MoS_2 edges.

REFERENCES

1 J. W. Gosselink, *CatTech,* 4 (1998) 127.
2 Auto-Oil II Programme, Comission of the European Communities, Com 626, 2000.
3 J. T. Miller, W. J. Reagan, J. A. Kaduk *et al., J. Catal.,* 193 (2000) 123.
4 US Patent 5851382, 1998; US Patent 5846406, 1998; US Patent 5770046, 1998.
5 B. Höhlein, P. Biedermann, T. Grube and R. Menzer, *J. Power Sources,* 84 (1999) 203.
6 O. Weisser and S. Landa, Sulphide Catalysts, their Properties and Applications, Pergamon Press, Oxford, 1973.
7 R. R. Chianelli, *Catal. Rev.-Sci. Eng.,* 26 (1984) 361.
8 R. Prins, V. H. J. de Beer and G. A. Somorjai, *Ibid.,* 31 (1989) 1.
9 B. C. Wiegand and C. M. Friend, *Chem. Rev.,* 92 (1992) 491.
10 H. Topsøe, B. S. Clausen and F. E. Massoth, Hydrotreating Catalysis, Springer, Berlin, 1996.
11 S. Eijsbouts, *Appl. Catal. A,* 158 (1997) 53.
12 P. L. J. Gunter, J. W. Niemantsverdriet, F. H. Ribeiro and G. A. Somorjai, *Catal. Rev.-Sci. Eng.,* 39 (1997) 77.
13 E. W. Kuipers, C. Laszlo and W. Wieldraaijer, *Catal. Lett.,* 17 (1993) 71.
14 R. M. van Hardeveld, P. L. J. Gunter, L. J. van Ijzendoorn *et al., Appl. Surf. Sci.,* 84 (1995) 339.
15 P. C. Thüne, Ph. D. Thesis, Eindhoven University of Technology, The Netherlands, 2000.
16 A. M. de Jong, V. H. J. de Beer, J. A. R. van Veen and J. W. Niemantsverdriet, *J. Phys. Chem.,* 100 (1996) 17722.
17 A. M. de Jong, H. J. Borg, L. J. van Ijzendoorn *et al., Ibid.,* 97 (1993) 6477.
18 J. C. Muijsers, Th. Weber, R. M. van Hardeveld *et al., J. Catal.,* 157 (1995) 698.
19 J. W. Niemantsverdriet, Spectroscopy in Catalysis: An Introduction, VCH, Weinheim,1993.
20 P. Arnoldy, J. A. M. van den Heijkant, G. D. de Bok and J. A. Moulijn, *J. Catal.,* 92 (1985) 35.
21 M. L. Vrinat, *Appl. Catal.,* 6 (1983) 137.
22 H. Schulz, M. Schon and N. Rahman, *Stud. Surf. Sci. Catal.,* 27 (1986) 201.
23 A. N. Startsev, *Catal. Rev.-Sci. Eng.,* 37 (1995) 353.
24 J. M. J. G. Lipsch and G. C. A. Schuit, *J. Catal.,* 15 (1969) 179.
25 J. Kraus and M. Zdrazil, *React. Kinet. Catal. Lett.,* 6 (1977) 475.
26 E. J. Markel, G. L. Schrader, N. N. Sauer and R. J. Angelici, *J. Catal.,* 116 (1989) 11.
27 B. T. Carvill and M. J. Thompson, *Appl. Catal.,* 75 (1991) 249.
28 E. J. M. Hensen, M. J. Vissenberg, V. H. J. de Beer *et al., J. Catal.,* 163 (1996) 429.
29 E. J. M. Hensen, H. J. A. Brans, G. M. H. J. Lardinois *et al., Ibid.,* 192 (2000) 98.
30 J. A. R. van Veen, E. Gerkema, A. M. van der Kraan and A. Knoester, *J. Chem. Soc. Chem. Commun.,* 22 (1987) 1684.
31 L. Coulier, V. H. J. de Beer, J. A. R. van Veen and J. W. Niemantsverdriet, *Topics in Catal.,* 13 (2000) 99.
32 Th. Weber, J. C. Muijsers, J. H. M. C. van Wolput *et al., J. Phys. Chem.,* 100 (1996) 14144.
33 J. F. Moulder, W. F. Stickle, P. E. Sobol and K. D. Bomben, Handbook of XPS, Perkin Elmer Corporation, Eden Prairie, MN, 1992.
34 N.-Y. Topsøe and H. Topsøe, *J. Catal.,* 84 (1983) 386.
35 S. P. A. Louwers and R. Prins, *Ibid.,* 133 (1992) 94.
36 J. A. R. van Veen, H. A. Colijn, P. A. J. M. Hendriks and A. J. van Welsenes, *Fuel Proc. Technol.,* 35 (1993) 137.
37 Th. Weber, J. C. Muijsers and J. W. Niemantsverdriet, *J. Phys. Chem.,* 99 (1995) 9194.
38 E. J. M. Hensen, V. H. J. de Beer, J. A. R. van Veen and R. A. van Santen, Submitted to *Catal. Lett.*
39 B. Scheffer, J. C. M. de Jonge, P. Arnoldy, and J. A. Moulijn, *Bull. Soc. Chim. Belg.,* 93 (1984) 751.
40 L. G. Silen and A. E. Martell, Stability Constants of Metal-Complexes, vol. 2, Chemical Society, London, 1964.
41 R. Cattaneo, T. Shido and R. Prins, *J. Catal.,* 185 (1999) 199.
42 R. Cattaneo, Th. Weber, T. Shido and R. Prins, *Ibid.,* 191 (2000) 225.